SCIENTIFIC REPORTS

OPEN

SUBJECT AREAS:

BIOPHYSICAL CHEMISTRY

ELECTRONIC PROPERTIES AND MATERIALS

Received
27 December 2013

Accepted
24 February 2014

Published
11 March 2014

Correspondence and requests for materials should be addressed to T.H.P. (thpark@snu.ac.kr) or J.J. (jsjang@plaza.snu.ac.kr)

* These authors contributed equally to this work.

Human dopamine receptor nanovesicles for gate-potential modulators in high-performance field-effect transistor biosensors

Seon Joo Park[1]*, Hyun Seok Song[2,3]*, Oh Seok Kwon[1,4], Ji Hyun Chung[2], Seung Hwan Lee[2], Ji Hyun An[1], Sae Ryun Ahn[2], Ji Eun Lee[5], Hyeonseok Yoon[5], Tai Hyun Park[2,6] & Jyongsik Jang[1]

[1]World Class University program of Chemical Convergence for Energy & Environment, School of Chemical and Biological Engineering, Seoul National University, 151-742, Korea, [2]School of Chemical and Biological Engineering, Seoul National University, Seoul 151-742, Korea, [3]Harvard–MIT Division of Health Sciences and Technology, Massachusetts Institute of Technology, 77 Massachusetts Ave., Cambridge, Massachusetts 02139, USA, [4]Department of Chemistry, Massachusetts Institute of Technology, 77 Massachusetts Avenue, Cambridge, Massachusetts 02139, USA, [5]Department of Polymer Engineering, Chonnam National University, Gwangju 500-757, Korea, [6]Advanced Institutes of Convergence Technology, Suwon 443-270, Korea.

The development of molecular detection that allows rapid responses with high sensitivity and selectivity remains challenging. Herein, we demonstrate the strategy of novel bio-nanotechnology to successfully fabricate high-performance dopamine (DA) biosensor using DA Receptor-containing uniform-particle-shaped Nanovesicles-immobilized Carboxylated poly(3,4-ethylenedioxythiophene) (CPEDOT) NTs (DRNCNs). DA molecules are commonly associated with serious diseases, such as Parkinson's and Alzheimer's diseases. For the first time, nanovesicles containing a human DA receptor D1 (hDRD1) were successfully constructed from HEK-293 cells, stably expressing hDRD1. The nanovesicles containing hDRD1 as gate-potential modulator on the conducting polymer (CP) nanomaterial transistors provided high-performance responses to DA molecule owing to their uniform, monodispersive morphologies and outstanding discrimination ability. Specifically, the DRNCNs were integrated into a liquid-ion gated field-effect transistor (FET) system via immobilization and attachment processes, leading to high sensitivity and excellent selectivity toward DA in liquid state. Unprecedentedly, the minimum detectable level (MDL) from the field-induced DA responses was as low as 10 pM in real- time, which is 10 times more sensitive than that of previously reported CP based-DA biosensors. Moreover, the FET-type DRNCN biosensor had a rapid response time (<1 s) and showed excellent selectivity in human serum.

Dopamine (DA) distribution in the mammalian brain has been widely studied since its discovery in the late 1950s[1]. DA is one of the most significant catecholamines and belongs to a biological group of excitatory chemical neurotransmitters[2–4]. It plays an important role in the functioning of the central nervous, renal, hormonal and cardiovascular systems. Abnormal control of DA concentrations in living bodies can result in several fatal diseases, such as Parkinson's and Alzheimer's diseases[5,6]. Therefore, the development of simple and rapid methodologies for detecting DA in human body fluids is extremely important in the field of precise clinical diagnosis and disease prevention. Field-effect transistor (FET)-based biosensors, which include silicon nanowire based on biotin-avidin binding[7], MPC-modified Si nanowire[8], and functionalized polysilicon nanowires[9] as transistors, have progressed in their ability to recognize DA. Although they showed high sensitivity to DA, these transistors had critical drawbacks such as slow response time and selectivity because the gate-modulating parts have no specificity to DA molecule. In addition, electrochemical methods[10–18] have also been widely introduced for DA analytical chemistry, demonstrated with the construction of diverse electrochemical electrodes (e.g., organic electrodes[16], CNT electrodes[14], and metal nanoparticle-based electrodes[19]) because DA is electroactive. However, the DA in biological liquids coexists with electroactive ascorbic acid and uric acid. These acids have a redox potential similar that of DA, resulting in main obstacles in fabricating high-performance DA biosensors with high sensitivity and selectivity[15,20]. Recent attempts to enhance DA sensing ability have involved modification of electrochemical electrodes to introduce functional groups that can only interact with the DA

molecule[3,21,22]. These methods based on surface engineering showed efficient strategies in DA detection; however critical technological problems such as post- or pre-treatments, low sensitivity due to small surface-to-volume ratios, low selectivity, and time-consuming responses still remain challenges.

A DA receptor naturally has high selectivity and specificity to DA and belongs to the family of G protein-coupled receptors (GPCRs), which are involved in important physiological processes, including neuronal transmission, sensory signaling, and hormone signaling[23–25]. Recently, GPCRs as recognizing elements in FET system allowed high selectivity for the detection of specific ligands and the development of biosensors based on nanomaterial-based geometries[24,26–29]. However, those protein-attached biosensors using GPCRs as recognition elements cannot mimic the GPCR-mediated intracellular signal transduction[30]. Furthermore, the functional study of GPCRs under cell-based assay, which is highly challenging masks for drug discovery and therapeutics, is often difficult because of low expression level and labor-intensive, time-consuming assay protocols[31–35]. Therefore, the new paradigm such as receptor-containing nanovesicles with functional GPCRs can be developed as gate-potential modulators in FET biosensing systems to overcome the limitations of conventional GPCR analytical methodologies for whole cell-like intracellular signal transduction[36,37]. In addition, the signal generated by the specific binding event of receptors and ligands can be amplified through the intracellular signaling in nanovesicles[36,37]. From this point of view, the realization of novel receptor-containing nanovesicles to target analytes is essential request to improve molecule sensing ability.

Owing to their unique chemical and physical properties, one-dimensional (1-D) electrical nanomaterials[11,38–43] such as wires[11,43,44], rods[45], belts, and tubes[29,38,39,41–43], play a key role as interconnectors and functional units in creating electronic, electrochemical, and optoelectronic devices on the nanometer scale. In particular, 1-D conducting polymer (CP) nanomaterials that have various advantages, such as facile functionalization[29,46–50], cost effectiveness[50], and biocompatibility[46,51,52], have been highlighted in various applications, including supercapacitors, solar cells, transistors, and sensors. Moreover, in the field of biosensors, 1-D CP nanomaterials integrated into sensing geometries, have demonstrated high-performance transducing capabilities due to their efficient charge transport along the long-axis direction[29,47,50]. In this regard, the utilization of 1-D CP nanomaterials in FET systems will pave the way for the next-generation electrical biosensor. In this study, we successfully fabricated a highly-sensitive, selective dopamine biosensor using DA receptor-containing uniform-particle-shaped nanovesicles-immobilized carboxylated poly(3,4-ethylene-dioxythiophene) (CPEDOT) NTs (DRNCNs). The nanovesicles as gate-potential modulator on CP transistor, which contain human DA receptor D1 (hDRD1), had highly uniform and monodispersive morphology, leading to the specific selectivity and enhanced sensitivity owing to their enlarged active sites compared with conventional CP-based DA biosensors. The DRNCN, which was attached to an interdigitated microelectrode array (IMA), was stably integrated into a liquid-ion gated FET geometry owing to the functional groups of CPEDOT and poly-D-lysine treatment, resulting in a high-performance FET-type DA biosensor. Field-induced real-time responses from the DRNCN-based biosensor were measured, which enabled highly sensitive and selective recognition of DA molecules at unprecedentedly low concentrations. Importantly, the minimum detection level (MDL) was *ca.* 10 pM, which is 10 times higher than that of conventional CP based-DA biosensors. Moreover, the FET-type biosensor based on DRNCN had a rapid response time (*ca.* 1 s) in phosphate-buffered saline (PBS, pH 7.4) and even displayed excellent selectivity in human serum consisting of various biological molecules. Based on these results, the excellent sensing capability of our FET geometry provides a new powerful platform to monitor the activity of GPCR upon ligand stimulation in real-time, which can be efficiently to drug discovery and therapeutics. To the best of our knowledge, this is first example of the introduction of nanovesicles as gate-potential modulators for high-performance liquid-ion gated FET-type DA biosensors.

Results

Fabrication of DRNCN geometry. Previously, we demonstrated a liquid-ion gated biosensor based on various biomolecule/CP nanotube hybrids[47,50,51]. To realize high-performance biosensors in the liquid state, the following critical key points should be considered: i) the stability of the transistors deposited on the electrode substrate in the liquid state, ii) a reliable connection between recognition elements and transistors, iii) specific binding events to target molecules at the active sites of the recognition elements, iv) enlarged surface-to-volume ratios at the nanoscale, and v) efficient charge transport along the long-axis direction. From these basic concepts, we successfully constructed a stable sensing geometry using DRNCN to specifically recognize DA in the liquid state. Fig. 1 illustrates the fabrication process of the DRNCN bridged between the electrode gaps. First, the surface of the IMA with gold electrode bands, which were prepared using a standard lithographic process on a glass substrate, was engineered using 3-aminopropyltrimethoxysilane (APS) to introduce the functional groups. The CPEDOT NTs were attached to the APS-treated IMA surface via covalent linkages between amino groups (-NH_2) on the substrate surface and the carboxylic groups (-COOH) of the CPEDOT NTs. Consecutively, uniform-particle-shaped nanovesicles were immobilized on the stable CPEDOT NT substrate using poly-D-lysine (PDL), a synthetic amino acid chain widely used as a coating to enhance cell attachment by its positive charge[36,53]. The nanovesicles derived from cells have same property to cell membranes and the treatment of PDL allowed efficient immobilization process. This approach of CPEDOT NTs provided an excellent sensing geometry, including smooth electrical pathways and efficient gating in the liquid state, compared with conventional non-covalent binding or physical adsorption methods.

Characterization of DRNCN geometry. For the construction of nanovesicles containing hDRD1, we developed an HEK-293 cell-line, stably expressing hDRD1 in the cell membranes. After the transfection of HEK-293 cells with the mammalian expression vector, pDsRed-N1, containing the DA receptor gene, cells stably expressing receptors were selected using G-418, while monitoring the red fluorescence from DsRed, which was fused in the C-terminus of hDRD1. Fig. 2a shows the fluorescence image of the HEK-293 stable cell line expressing the DA receptor. Red fluorescence was observed from every cell, demonstrating stable expression of the DA receptor from the HEK-293 cells. We also carried out a Ca^{2+} signaling assay using the calcium indicator Fura2-AM to confirm the activity of the cells. Fig. 2b shows the fluorescence intensity from the cells with the addition of different concentrations of DA. The dose-response profile showed a calcium ion influx into the cytoplasm, triggered by the specific binding of the DA receptor and DA; this indicated successful construction of the cell line expressing DA receptors. Additionally, the further measurement of the Ca^{2+} signaling assay using different neurotransmitters revealed that the DA receptor cell lines only responded to DA, among various neurotransmitters, and were highly selective to DA (Fig. S1).

A cell-line, stably expressing hDRD1, was constructed and treated with cytochalasin B to destabilize the cell membrane by degrading the cytoskeleton in the cells. hDRD1 emitting nanovesicles were obtained through gentle agitation of the cells[36,37]. These nanovesicles possessed signaling capability for hDRD1-mediate signal transduction, such as G protein adenylyl cyclase and ion channels. The nanovesicles were then immobilized on a CPEDOT NT substrate using poly-D-lysine (PDL). Nanovesicles containing hDRD1 were

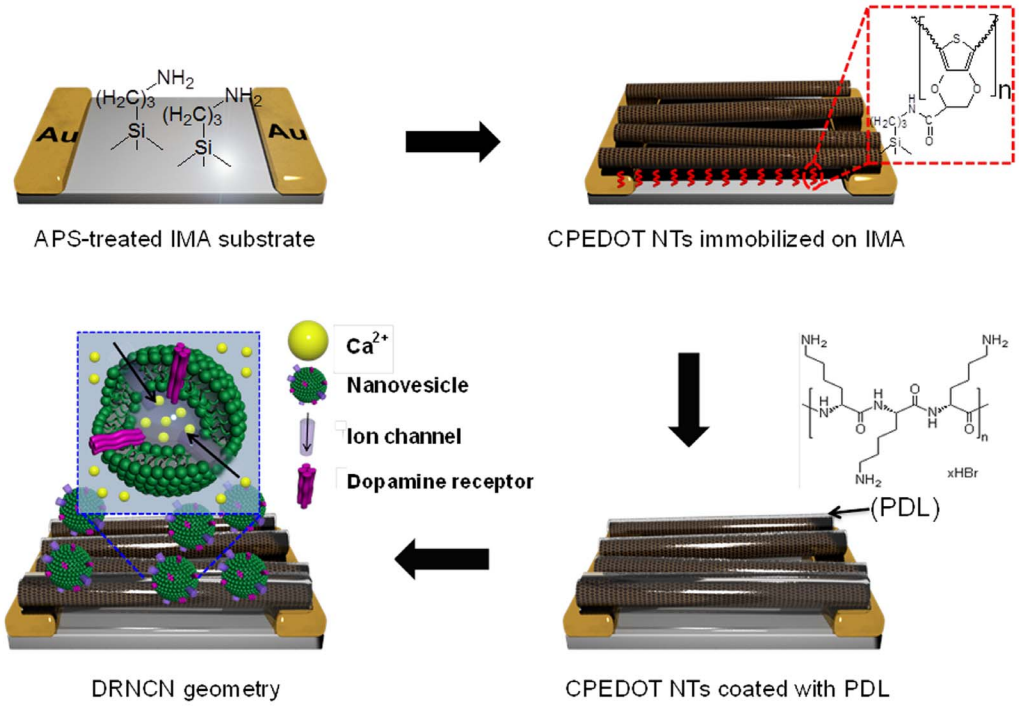

Figure 1 | **Schematic illustrations of construction steps for DRNCN geometry.**

produced by a cytochalasin B treatment that degraded the cytoskeleton, making the cell membrane unstable. The nanovesicles can be budded out from the cells with gentle agitation and centrifugation. Fig. 2c shows Western blot analysis of the membrane fraction of the HEK-293 stable cell-line and nanovesicles using an antibody against a HA-tag fused in the N-terminus of hDRD1. The bend observed from both the membrane fraction of the cells and the nanovesicles corresponded to the molecular weight of the DA receptor, as a DsRed fusion protein. This result clearly indicated that the DA receptor was successfully expressed from the cell membrane and that the nanovesicles contained a sufficient amount of hDRD1. The formation of nanovesicles was confirmed by field-emission scanning electron microscopy (FE-SEM) image analysis (Fig. 2d). The nanovesicles exhibited a well-defined spherical shape, with a uniform diameter

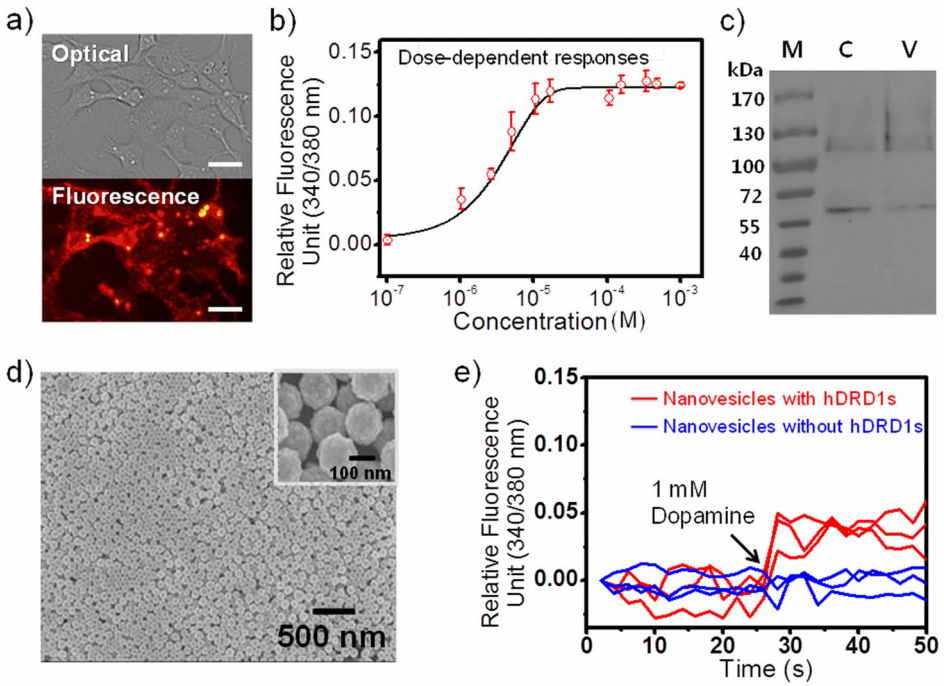

Figure 2 | **Construction of stable cell-line expressing hDRD1 and nanovesicles.** (a) Optical and fluorescence image of HEK-293 cells stably expressing hDRD1 (scale bar: 50 μm). (b) Ca^{2+} signaling assay of HEK293 cells stably expressing hDRD1 upon various concentrations of DA. (c) Western blot analysis of each membrane fractions of cells and nanovesicles expressing hDRD1 using anti-HA antibody (M: marker, C: cells and V: nanovesicles). (d) SEM image of nanovesicles derived from HEK-293 cells stably expressing hDRD1. (e) Real-time measurement of Ca^{2+} influx into nanovesicles containing hDRD1 upon the addition of 1 mM dopamine.

of 100 ~ 150 nm. Real-time fluorescence intensity was used to measure the activity of nanovesicles containing hDRD1 as a function of added DA; a Ca^{2+} indicator was used with Fura2-AM-loaded nanovesicles. Fig. 2e shows an immediate increase in the fluorescence intensity as DA was added. Note that calcium influx can occur due to the DA receptor-mediated signaling triggered by the specific binding of DA and the DA receptor protein. The nanovesicles containing DA receptor exhibited whole cell-like hDRD1-mediated intracellular signaling. The uniform sphere was a suitable size for integration with a CPEDOT-FET sensor platform and allowed for reproducible measurements of DA.

Previously, we synthesized various 1-D CP nanomaterials, such as polypyrrole NTs, PEDOT nanorods, and co-axial PEDOT nanofibers, which exhibited excellent transistor characterisitics for chemical and biological sensors[38,40-42]. From our previous studies, we determined that it was necessary to attach the transistors to the electrode substrate to achieve sensor stability. The movement of the transistors causes inter-contact resistances and loss of the transistors via each washing step, resulting in degradation of the sensing performance. Therefore, in this study, a copolymerization process was used to functionalize the PEDOT NTs with carboxylic groups (-COOH) to immobilize the transistor on an interdigitated microelectrode arrays (IMA) (Figure S2 in supporting information)[38,40–42]. Specifically, a soft template of the reverse-cylindrical micelle phase was formed by sodium bis(2-ethylhexyl) sulfosuccinate (AOT), allowing iron cation adsorption. Subsequently, a the mixture of 3,4-ethylenedioxythiophene (EDOT) and 2,3-dihydrothieno(3,4-b)[1,4]dioxine-2-carboxylic acid (EDOT-COOH) was added to the micelle phase, leading to the successful fabrication of the CPEDOT NTs via chemical oxidation polymerization.

The IMA electrodes were modified by surface engineering with APS. This procedure is described in the following.

$$\text{Hydrolysis}: \ H_2N(CH_2)_3Si(OCH_3)_3 + 3H_2O \rightarrow H_2N(CH_2)_3Si(OH)_3 + 3CH_3OH \quad (1)$$

$$\text{Condensation}: \ H_2N(CH_2)_3Si(OH)_3 + 3OH - \text{glass substrate} \rightarrow H_2N(CH_2)_3Si(O)_3 - \text{glass substrate} \quad (2)$$

The APS-treated IMA electrode substrate was characterized by X-ray photoemission spectroscopy (XPS) and compared with a pristine glass substrate (Fig. 3a). The survey scan spectrum of the APS-treated substrate had the principal C 1s, O 1s, Si 2p, and N 1s core levels; no significant N 1s peak in the pristine IMA substrate. The N 1s peak (3.8%), which consisted of peaks at 390.3 (non-protonated amine groups), 400.5, and 401.8 eV (protonated amine groups), was clearly observed in the APS-treated substrate (Fig. 3b)[46]. Therefore, the amine-functionalized substrate can be utilized as a substrate support for assembling the biosensing device.

To design a stable transistor on the APS-treated IMA, the CPEDOT NTs were functionalized by co-polymerization. The carboxylic group (-COOH) of the CPEDOT NTs was also confirmed by XPS analysis. The survey spectrum of the CPEDOT NTs indicated the presence of principal C 1s, O 1s, and S core levels, with no evidence of impurities (Fig. S3). The C 1s peak (70.5%) was measured for the CPEDOT NTs and consisted of four components centered at 284.5, 285.85, 287.05, and 288.59 eV corresponding to C=C, C-C, C-O-C, and O-C=O or C=O molecules, respectively (Fig. 3c). The carboxylic groups of the CPEDOT NTs actively participated in the condensation reaction to build covalent bonds between the CPEDOT NTs and IMA substrate, using an efficient condensing agent, 4-(4,6-dimethoxy-1,3,5-triazin-2-yl)-4-methylmorpholinium chloride (DMT-MM), leading to the formation of stable CPEDOT NT transistors on the IMA. The process of this chemical reaction is described below.

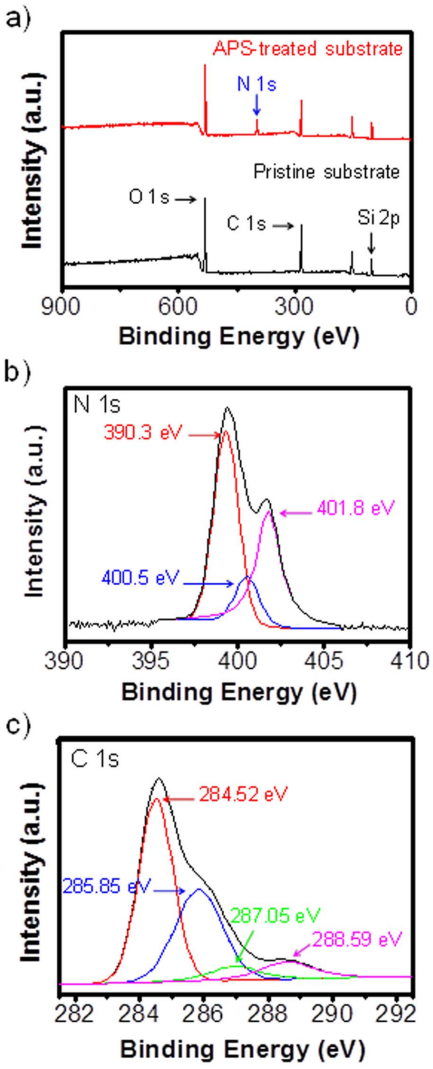

Figure 3 | Characterization of sensing substrate. (a) XPS spectra of the IMA substrate before and after aminosilane treatment. (b) XPS N 1s spectrum of aminosilane-treated IMA substrate. (c) XPS C 1s spectrum of the CPEDOTs.

$$\text{Condensation}: \ \text{CPEDOT} - \text{COOH} + H_2N(CH_2)_3Si(O)_3 - \text{glass substrate} \rightarrow \text{CPEDOT} - \text{CONH}(CH_2)_3Si(O)_3 - \text{glass substrate} \quad (3)$$

Consecutively, the hDRD1-containing uniform-particle-shaped nanovesicles were immobilized on the PDL-deposited CPEDOT attached to the IMA. PDL not only immobilizes the biomolecules on the transistor, but it can also provide the passivation to prevent direct binding between the target molecules and transducer. FE-SEM was used to observe the DRNCN attached to the IMA substrate. Fig. 4 shows FE-SEM images before (Fig. 4a) and after (Fig. 4b) the introduction of the nanovesicles on CPEDOT NTs. The close-packed arrays of uniform nanovesicles, designed using the charge interaction between the nanovesicles and PDL, were clearly observed on the PDL-coated CPEDOT NT substrate.

Electrical properties of liquid-ion gated FET-type DRNCN. To confirm the electrical properties of the DRNCN sensing geometry, we obtained the current-voltage (I-V) curves for DRNCN. Fig. 5a displays the I-V characteristics of the IMA surface-attached CPEDOT, before and after nanovesicle immobilization. The I-V changes of the PDL-coated CPEDOT substrate were continuously maintained with linear curves over a voltage range from −10 to

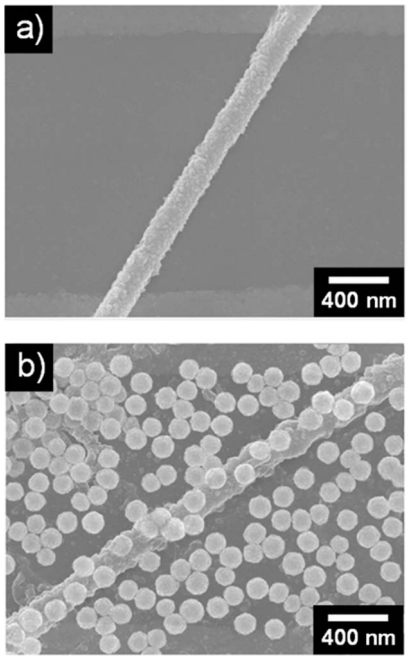

Figure 4 | **FE-SEM images before (a) and after (b) the introduction of the nanovesicles on CPEDOT NTs.**

10 mV, demonstrating stable ohmic behavior of the nanomaterials on the IMA substrate. Moreover, to identify the importance of PDL, a CPEDOT substrate without PDL was prepared as a control experiment, with the addition of nanovesicles. The dI/dV value of the nanovesicle/PDL/CPEDOT NTs of 0.08 was two times lower than that of the nanovesicle/CPEDOT NTs without PDL (0.17), enhancing the amount of nanovesicles immobilized on the PDL/CPEDOT NTs. The existence of the PDL critically affected sensing performance, due to the accumulation of sensing elements.

To utilize DRNCN as the signal transducing component of the biosensor, a liquid-ion gated FET system was constructed by the surrounding PBS (pH 7.4) as the electrolyte. Generally, in biosensors, the analytes exist in a liquid state and require optimal environmental conditions. High-performance biosensors require stable transducers with excellent electrical properties that can induce significant binding events between the transducer and sensing elements in the liquid state. Therefore, a liquid-ion gated FET system was introduced in this study. Liquid-ion gating allows for a significant contact area for on the wide-range areas of the DRNCN via a controllable gate electrode in the electrolyte and operates as a signal amplifier to enhance the sensing performance of sensitively resistive sensors. Fig. 5b shows a schematic diagram of a liquid-ion gated FET-type DA biosensor based on DRNCN. The source (S) and drain (D) electrodes were designed from IMA; a reference electrode was also immersed in the electrolyte. A gate potential (V_g) was applied between the reference electrode and the drain electrode through the liquid-ion solution. Fig. 5c shows the out-put characteristics of the FET-type DRNCN biosensor at room temperature. The drain-to-source current (I_{ds}) negatively increased with negatively increasing gate voltage; this was induced by an increment in the oxidation level of the CP chains, indicating clearly p-type behavior (hole-transporting). The binding events between the DA molecules and DRNCN bridged on source and drain of IMA can be monitored by measuring the current output under controlled gating voltages. The FET-type DA biosensor produced rapid real-time responses with high sensitivity and selectivity.

Real-time responses of liquid-ion gated FET-type DRNCN DA biosensor. To evaluate the sensing characteristics of the DRNCN-based FET-type DA biosensors surrounded with PBS containing

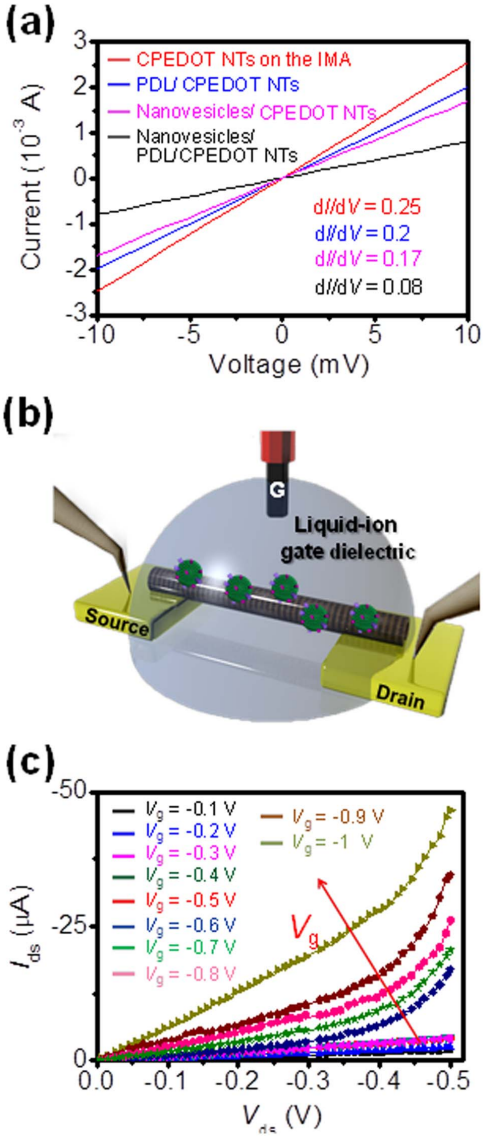

Figure 5 | (a) Current-voltage (*I-V*) curves of the IMA surface-attached CPEDOT before and after the immobilization of nanovesicles. (b) Schematic illustration of the liquid-ion gated FET-type DA biosensor using DRNCN. (c) Output curves of DRNCN FET (V_g was from −0.1 to −1 V in a step of −0.1 V and V_{ds} scan rate was −5 mV s^{-1}).

2 mM Ca^{2+}, the field-induced Ids was measured as a function of DA concentration for Vds = −50 mV, under a low operating voltage (Vg = −50 mV). The principal function of the DA receptor-containing nanovesicle was to bind with the molecules. The signal induced from the binding event activated a G protein and Ca^{2+} channels following the cAMP pathway in the nanovesicle (Fig. S4). The activation of the Ca^{2+} channel triggered the influx of Ca^{2+} into the nanovesicles, which accumulated the potential of the nanovesicle immobilized on the PDL/CPEDOT substrate. The introduction of Ca^{2+} into the uniform-particle-shaped nanovesicle can affected the charge carrier density on the surface of the CPEDOT NTs, indirectly. Fig. 6a displays the real-time response of the FET-type DA biosensor, after the introduction of various concentrations of DA. The FET-type biosensor based on DRNCN exhibited a concentration-dependent decrement in Ids upon exposure to DA molecules. It can be explained by the reduction of the charge carriers (holes) due to the accumulation Ca^{2+} on the CPEDOT NTs. The specific binding of hDRD1/DA promotes activity of the Ca^{2+} channel, resulting in the generation of positive point charges in

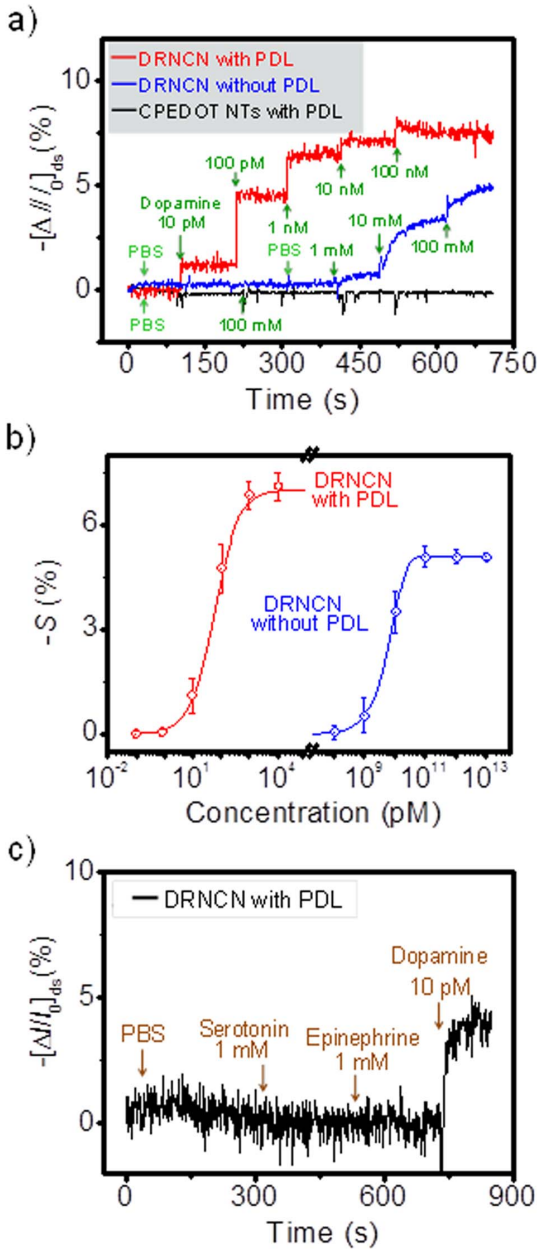

Figure 6 | (a) Real-time responses with normalized current changes ($\Delta I/I_0$) and (b) calibration curves of DRNCN toward various DA concentrations (S indicates the normalized current change). (c) Selective responses of the DA biosensor using DRNCN toward non-target neurotransmitters (PBS, 1 mM Serotonin, and 1 mM Epinephrine) and dopamine (10 pM DA).

the liquid-ion gate dielectric near the CPEDOT NT surface. Therefore, the positively charged carriers in the CPEDOT NTs channel decreased, leading to the decreasing current. From this sensing mechanism, no significant signal was obtained from the pristine CPEDOT NTs treated with PDT as a control experiment. In contrast, the DA biosensors based on DRNCN exhibited a highly sensitive response. Moreover, the DRNCN with PDL showed more sensitive responses than those of the DRNCN without PDL due to nanovesicle immobilization (Fig. 6b). Unprecedentedly MDL of the FET-type DA biosensors using DRNCN was ca. 10 pM, which is approximately 1 ~ 2 orders of magnitude lower than that of various conventional CP-based DA biosensors (Table S1). In all of the measurements, the FET-type DA biosensors exhibited a rapid response time of less than 1 s, because receptor signaling in sensory

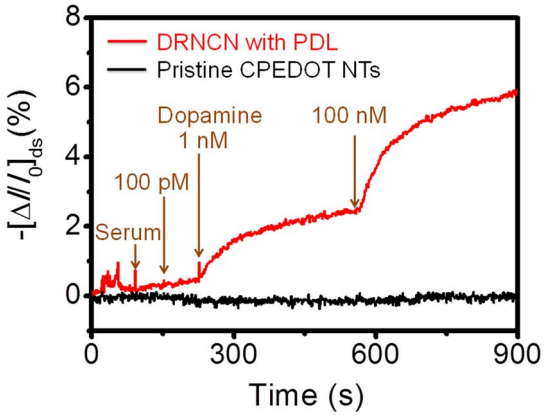

Figure 7 | **Selective response of FET-type DRNCN biosensor toward DA molecules in human serum.**

transduction is relatively fast on the order of milliseconds. Interestingly, the sensitivity from DA biosensors can be affected by the concentrations of nanovesicles, while the response time showed slight changes (Fig. S5). Fig. 5c shows the highly selective responses of the FET-type DA biosensor toward molecules containing similar structures. No significant changes in I_{ds} were observed upon the addition of non-target neurotransmitters and precursor, including serotonin, epinephrine, tyrosine, phenethylamine, and norepinephrine; however, a change in I_{ds} was clearly evident with the addition of DA, for concentrations as low as 10 pM (Fig. S6). Thus, a high-performance DA biosensor can be created by DRNCN through the immobilization processes.

Discussion

Because the DA molecule coexists with various biomolecules in the living body, the biosensor must have the ability to precisely distinguish DA molecules. Samples with human serum were prepared to confirm the DA selectivity of the FET-type DRNCN-based biosensors under similar living conditions. The selective responses from DRNCN were monitored by changes in the current upon sample exposure. No significant signal was observed when human serum and PBS were added to the DA biosensor. In contrast, the responses from DRNCN were clearly evident (Fig. 7). The FET-type DA biosensor showed a significant signal and had a higher MDL (1 nM DA) than that shown in Fig. 6a (MDL: 10 pM); this was attributed to interrupting biomolecules in the human serum, and the excellent selectivity in various biomolecules was successfully demonstrated. Previous reports have suggested that the concentration of DA in the blood fluid of the caudate nucleus is in the nanomolar range for Parkinson's disease patients; for a healthy individual, the DA concentration is in the micromolar range[20,54–56]. Note that, the detection limit of our DA biosensor is sufficient for the detection of DA in human blood, suggesting the application of our biosensor to the diagnosis of Parkinson's disease.

In summary, we successfully fabricated a liquid-ion gated FET-type DA biosensor based on the hDRD1-containing uniform-particle-shaped nanovesicle-immobilized carboxylated poly(3,4-ethylene-dioxythiophene) NTs (DRNCN). The attachment of CPEDOT on IMA produced a stable transducer in a liquid state. Moreover, the immobilization of nanovesicles as gate-potential modulator on the CPEDOT NTs by PDL resulted in a highly stable FET, suitable for sensing devices. Field-induced responses from the DRNCN geometry demonstrated high-performance sensing properties at unprecedentedly low concentrations (*ca.* 10 pM). Moreover, the DA biosensor based on DRNCN was able to discriminate DA from nontarget molecules with similar structures. Importantly, the excellent selectivity of the FET-type DA biosensor in human serum

was also demonstrated. Therefore, the designed FET-type DA biosensor using DRNCN could be utilized as transducer for high-performance sensing applications, leading to rapid and accurate methodologies for disease diagnosis and management. Furthermore, our study offers an efficient tool for monitoring GPCR activity upon ligand stimulation. This suggests its use for the detection of GPCR-mediated intracellular signaling, which would replace the previous the high-cost and labor-intensive cell-based assays currently used.

Methods

Materials. 3,4-ethylenedioxythiophene (EDOT) and 2,3-Dihydrothieno(3,4-b)[1,4]dioxine-2-carboxylic acid (EDOT carboxylic acid) were obtained from Sigma-Aldrich. Sodium bis(2-ethylhexyl)-sulfosuccinate (AOT; Aldrich, 98%) and hexane (Aldrich, 99%) were purchased from Aldrich. For specific material information, see the Supporting Information section.

Cloning. hDRD1 gene (GeneBank N0. NC000005.9) fused with 3HA-tag at the N-terminus of hDRD1 was amplified by PCR with primers (5′ AAG GTA CCA TGT ACC CAT ACG ATG TTC C 3′, 5′ AAC TCG AGG GTT GGG TGC TGA CC 3′) using pcDNA3.1 containing hDRD1 cDNA and 3HA-tag. Amplified PCR product was inserted into in-frame between the KpnI and XhoI of restriction sites of a multiple cloning site in a mammalian expression vector pDsRed-N1 using ligation kit (Takara).

Construction of HEK-293 cell-line stably expressing hDRD1. Human embryonic kidney-293 (HEK-293) cells were cultured in Dulbecco's modified Eagle medium (DMEM) supplemented with 10% fetal bovine serum and 0.5% penicillin-streptomycin (Gibco) at 37°C under 5% CO_2 and transfected with pDsRed-3HA-hDRD1 using Lipofectamine 2000 (Invitrogen). Transfected ells were transferred to the culture media containing G-418 (1 mg/mL) and changed to fresh media every 3 days. G-418 resistant cells formed colonies by culture for 10 days and the colonies which have red fluorescence were picked up and transferred into fresh media containing G-418. HEK-293 cells stably expressing hDRD1 were cultured continuously and used for the production of nanovesicles.

Construction of nanovesicles from HEK-293 cell-line stably expressing hDRD1. Adherent hDRD1 expressing HEK-293 cells were incubated in serum-free DMEM containing cytochalasin B (20 μg/ml) at 37°C with 300 rpm agitation. After the incubation, Cells and cell debris were separated with centrifugation (200 g for cells, 2,000 g for cell debris). Suspended nanovesicles were collected with centrifugation (15,000 g) and resuspended in PBS (pH 7.4) containing protease inhibitor cocktail (Sigma).

Western blot analysis. The cells or nanovesicles containing hDRD1 were lysed by weak sonication and the membrane fractions were collected by centrifugation (15,000 g, 30 min). The pellet fractions were resuspended in PBS buffer and mixed with SDS sample buffer containing10% sodium dodecyl sulfate, 10% β-mercaptonethanol, 0.3 M Tris-HCl (pH 6.8), 0.05% bromophenol blue and 50% glycerol. Each samples were boiled at 100°C for 5 min and same volumes of samples were loaded onto 10% PAGE gels (Laemmli) and electrophoresed at 80 V. Proteins in the SDS-PAGE gel were transferred to nitrocellulose membranes and incubated for 2 h with 5% skim milk in PBS-T (PBS containing 0.1% Tween-20) for blocking. After the blocking, the membrane was incubated with anti-HA antibody (from mouse, 1 : 1,000 dilution, Santa Cruz) in 1% skim milk in PBS-T for 2 hr at room temperature with gentle rocking and then washed with PBS-T (10 min, 5 times). HRP-conjugated anti-mouse antibody (1 : 2,00 dilution with 5% skim milk in PBS-T: GE Healthcare) was then incubated with anti-HA antibody treated membrane for 2 h at room temperature with gentle rocking and washed with PBS-T (10 min, 5 times). Western blot was performed using an ECL kit (GE Healthcare).

Intracellular Ca^{2+} assay. 5 μM Fura 2-acetoxymethyl (AM) (calcium indicator, Invitrogen) was loaded into HEK-293 cells stably expressing hDRD1 with the incubation in an imaging buffer (in mM: NaCl 140, KCl 5, $MgCl_2$ 1, $CaCl_2$ 2, HEPES 10, Glucose 10, 0.1% Pluronic F-127, pH 7.4) at 37°C for 30 min and then washed with the imaging buffer. The cleavage of the AM ester group was allowed by the incubation for 1 h at 37°C. The fluorescence signal was measured at 510 nm by dual excitation at 340 nm and 380 nm using a spectrofluorophotometer (Tecan) upon the addition of various concentrations of neurotransmitters and 100 μM of ATP. For intracellular Ca^{2+} assay of nanovesicles, hDRD1 expressing nanovesicles were produced from Fura 2-AM loaded HEK-293 cells stably expressing hDRD1 according to the process described above. The Fure 2-AM loaded nanovesicles were immobilized on poly-D-lysine treated 96-wells plate with the incubation at 37°C for 2 h.

Fabrication of CPEDOT. Carboxylated PEDOT (CPEDOT) nanomaterials with a diameter of *ca.* 200 ~ 180 nm were fabricated by chemical oxidation co-polymerization by AOT micelle templates. AOT was dissolved in hexane at a concentration of 3×10^{-1} M, and then 5 M of aqueous $FeCl_3$ solution was added into the AOT/hexane solution. The volume ratio of aqueous $FeCl_3$ solution to hexane was 3×10^{-2}. Subsequently, 0.25 mmol of EDOT-COOH was dissolved into 7.5 mmol of EDOT monomer at an EDOT-COOH/EDOT molar ratio of 1/30. The mixture was injected by drop-wise into the AOT/hexane solution. The chemical oxidation co-polymerization was proceeded for 5 h at 20°C. The final products were thoroughly washed with ethanol to remove other residual reagents and dried in a vacuum oven at room temperature.

Fabrication of liquid-ion gated FET-type DRNCN geometry. To fabricate liquid-ion gated FET-type DRNCN sensing geometry, in the first stage, the surface of the IMA was functionalized with amino groups by immersion in 5 wt% aq. aminosilane (3-aminopropyltrimethoxysilane, APS) for 6 h. A mixture of 0.1 wt% aq. CPEDOT NTs solution (40 μL) and 0.1 wt% aq. 4-(4,6-dimethoxy-1,3,5-triazin-2-ly)-4-methylmorpholinium chloride solution (DMT-MM, 40 μL) were used to treat the amino group-modified IMA surface for over 12 h. The resulting CPEDOT-attached IMA substrate was washed with distilled water. The surface of the CPEDOT NT substrate was coated with 0.1 mg mL-1 poly-D-lysine (PDL) solution and incubated at 25°C for 2 h to electrostatically enhance the immobilization of nanovesicles on the CPEDOT NT substrate. Then, a 1 μL droplet of nanovesicle solution (1 mg/mL) was placed on the PDL-coated CPEDOT NT substrate, and this was incubated at 4°C for 4 h. Finally, the prepared nanovesicle-immobilized PDL/CPEDOT NT substrate was surrounded by PBS (pH 7.4) as an electrolyte, leading to the successful fabrication of the liquid-ion gated FET-type DRNCN geometry.

SEM preparation of nanovesicles. To retain the shape of the nanovesicles for SEM analysis, liquids in nanovesicles were dried by lyophilization. The lyophilization process was performed by similar method described in our previous work[36]. Briefly, cell-derived nanovesicles were doped on a glass surface or immobilized on CPEDOT NT substrate by the treatment with PDL. Samples were then lyophilized by freeze-drying. After the lyophilization, nanovesicles were coated with platinum by sputtering.

Instrumentation. Keithley 2400 sourcemeter and a Wonatech WBCS 3000 potentiostat was utilized for measuring all electrical signals induced from binding events. A solution chamber (200 μL volume) was introduced for solution-based measurements of FET device. The current change was normalized as $\Delta I/I_0 = (I - I_0)/I_0$, where I_0 is the initial current and I is the measured value in a real-time, respectively.

1. Wightman, R. *et al.* Temporally resolved catecholamine spikes correspond to single vesicle release from individual chromaffin cells. *Proc. Nat. Acad. Sci.* **88**, 10754–10758 (1991).
2. Laviolette, S. R. Dopamine modulation of emotional processing in cortical and subcortical neural circuits: evidence for a final common pathway in schizophrenia? *Schizophrenia Bull.* **33**, 971–981 (2007).
3. Maue, M. & Schrader, T. A color sensor for catecholamines. *Angew. Chem.* **117**, 2305–2310 (2005).
4. Wickens, J. R., Horvitz, J. C., Costa, R. M. & Killcross, S. Dopaminergic mechanisms in actions and habits. *J. Neurosci.* **27**, 8181–8183 (2007).
5. Ahlskog, J. E. Beating a dead horse dopamine and Parkinson disease. *Neurology* **69**, 1701–1711 (2007).
6. Tang, T.-S., Chen, X., Liu, J. & Bezprozvanny, I. Dopaminergic signaling and striatal neurodegeneration in Huntington's disease. *J. Neurosci.* **27**, 7899–7910 (2007).
7. Li, B.-R. *et al.* Biomolecular recognition with a sensitivity-enhanced nanowire transistor biosensor. *Biosens. Bioelectron.* **45**, 252–259 (2013).
8. Li, B.-R. *et al.* An Ultrasensitive nanowire-transistor biosensor for detecting dopamine release from living PC12 cells under hypoxic stimulation. *J Am. Chem. Soc.* **135**, 16034–16037 (2013).
9. Lin, C.-H. *et al.* Ultrasensitive detection of dopamine using a polysilicon nanowire field-effect transistor. *Chem. Commun.* 5749–5751 (2008).
10. Fabre, B. & Taillebois, L. Poly (aniline boronic acid)-based conductimetric sensor of dopamine. *Chem. Commun.* 2982–2983 (2003).
11. Gao, X. P., Zheng, G. & Lieber, C. M. Subthreshold regime has the optimal sensitivity for nanowire FET biosensors. *Nano Lett.* **10**, 547–552 (2009).
12. Goyal, R. N., Gupta, V. K., Bachheti, N. & Sharma, R. A. Electrochemical sensor for the determination of dopamine in presence of high concentration of ascorbic acid using a fullerene-C60 coated gold electrode. *Electroanalysis* **20**, 757–764 (2008).
13. Mao, Y., Bao, Y., Gan, S., Li, F. & Niu, L. Electrochemical sensor for dopamine based on a novel graphene-molecular imprinted polymers composite recognition element. *Biosens. Bioelectron.* **28**, 291–297 (2011).
14. Min, K. & Yoo, Y. J. Amperometric detection of dopamine based on tyrosinase–SWNTs–Ppy composite electrode. *Talanta* **80**, 1007–1011 (2009).
15. Sun, C.-L. *et al.* Microwave-assisted synthesis of a core–shell MWCNT/GONR heterostructure for the electrochemical detection of ascorbic acid, dopamine, and uric acid. *ACS Nano* **5**, 7788–7795 (2011).
16. Tang, H., Lin, P., Chan, H. L. & Yan, F. Highly sensitive dopamine biosensors based on organic electrochemical transistors. *Biosens. Bioelectron.* **26**, 4559–4563 (2011).

17. Wei, M. *et al.* Selective determination of dopamine on a boron-doped diamond electrode modified with gold nanoparticle/polyelectrolyte-coated polystyrene colloids. *Adv. Funct. Mater.* **18**, 1414–1421 (2008).
18. Gao, F. *et al.* Highly sensitive and selective detection of dopamine in the presence of ascorbic acid at graphene oxide modified electrode. *Sens. Actu. B* **186**, 380–387 (2013).
19. Atta, N. F. & El-Kady, M. F. Novel poly (3-methylthiophene)/Pd, Pt nanoparticle sensor: synthesis, characterization and its application to the simultaneous analysis of dopamine and ascorbic acid in biological fluids. *Sens. Actu. B* **145**, 299–310 (2010).
20. Ali, S. R. *et al.* A nonoxidative sensor based on a self-doped polyaniline/carbon nanotube composite for sensitive and selective detection of the neurotransmitter dopamine. *Anal. Chem.* **79**, 2583–2587 (2007).
21. Łuczak, T. Preparation and characterization of the dopamine film electrochemically deposited on a gold template and its applications for dopamine sensing in aqueous solution. *Electrochim. Acta* **53**, 5725–5731 (2008).
22. Secor, K. E. & Glass, T. E. Selective amine recognition: development of a chemosensor for dopamine and norepinephrine. *Org. Lett.* **6**, 3727–3730 (2004).
23. Beck-Sickinger, A. G. & Budisa, N. Genetically encoded photocrosslinkers as molecular probes to study G-protein-coupled receptors (GPCRs). *Angew. Chem. Int. Edit.* **51**, 310–312 (2012).
24. Park, S. J. *et al.* Ultrasensitive flexible graphene based field-effect transistor (FET)-type bioelectronic nose. *Nano letters* **12**, 5082–5090 (2012).
25. Rasmussen, S. G. *et al.* Crystal structure of the human β_2 adrenergic G-protein-coupled receptor. *Nature* **450**, 383–387 (2007).
26. Kim, B. *et al.* Highly selective and sensitive detection of neurotransmitters using receptor-modified single-walled carbon nanotube sensors. *Nanotechnology* **24**, 285501 (2013).
27. Kim, T. H. *et al.* "Bioelectronic super-taster" device based on taste receptor-carbon nanotube hybrid structures. *Lab Chip* **11**, 2262–2267 (2011).
28. Kwon, O. S. *et al.* Ultrasensitive and selective recognition of peptide hormone using close-packed arrays of hPTHR-conjugated polymer nanoparticles. *ACS Nano* **6**, 5549–5558 (2012).
29. Song, H. S. *et al.* Human taste receptor-functionalized field effect transistor as a human-like nanobioelectronic tongue. *Nano Lett.* **13**, 172–178 (2013).
30. Ferguson, S. S. Evolving concepts in G protein-coupled receptor endocytosis: the role in receptor desensitization and signaling. *Pharmacol. Rev.* **53**, 1–24 (2001).
31. Chou, K.-C. Prediction of G-protein-coupled receptor classes. *J. Prot. Res.* **4**, 1413–1418 (2005).
32. Michalke, K. *et al.* Mammalian G-protein-coupled receptor expression in *Escherichia coli*: I. High-throughput large-scale production as inclusion bodies. *Anal. Biochem.* **386**, 147–155 (2009).
33. Sarramegna, V., Muller, I., Milon, A. & Talmont, F. Recombinant G protein-coupled receptors from expression to renaturation: a challenge towards structure. *Cell. Mol. Life Sci.* **63**, 1149–1164 (2006).
34. Sarramegna, V., Talmont, F., Demange, P. & Milon, A. Heterologous expression of G-protein-coupled receptors: comparison of expression systems from the standpoint of large-scale production and purification. *Cell. Mol. Life Sci.* **60**, 1529–1546 (2003).
35. Thomsen, W., Frazer, J. & Unett, D. Functional assays for screening GPCR targets. *Curr. Opin. Biotech.* **16**, 655–665 (2005).
36. Jin, H. J. *et al.* Nanovesicle-based bioelectronic nose platform mimicking human olfactory signal transduction. *Biosens. Bioelectron.* **35**, 335–341 (2012).
37. Park, J. *et al.* A bioelectronic sensor based on canine olfactory nanovesicle–carbon nanotube hybrid structures for the fast assessment of food quality. *Analyst* **137**, 3249–3254 (2012).
38. Ding, M. & Star, A. Selecting fruits with carbon nanotube sensors. *Angew. Chem. Int. Edit.* **51**, 7637–7638 (2012).
39. Esser, B., Schnorr, J. M. & Swager, T. M. Selective detection of ethylene gas using carbon nanotube-based devices: utility in determination of fruit ripeness. *Angew. Chem. Int. Edit.* **51**, 5752–5756 (2012).
40. Knopfmacher, O. *et al.* Nernst limit in dual-gated Si-nanowire FET sensors. *Nano Lett.* **10**, 2268–2274 (2010).
41. Lobez, J. M. & Swager, T. M. Radiation detection: Resistivity responses in functional poly (olefin sulfone)/carbon nanotube composites. *Angew. Chem.* **122**, 99–102 (2010).
42. Star, A., Gabriel, J.-C. P., Bradley, K. & Grüner, G. Electronic detection of specific protein binding using nanotube FET devices. *Nano Lett.* **3**, 459–463 (2003).
43. Zheng, G., Gao, X. P. & Lieber, C. M. Frequency domain detection of biomolecules using silicon nanowire biosensors. *Nano Lett.* **10**, 3179–3183 (2010).
44. Ahn, J.-H. *et al.* Double-gate nanowire field effect transistor for a biosensor. *Nano Lett.* **10**, 2934–2938 (2010).
45. Dong, H. *et al.* Nanowire crystals of a rigid rod conjugated polymer. *J. Am. Chem. Soc.* **131**, 17315–17320 (2009).
46. Garnier, F., Youssoufi, H. K., Srivastava, P. & Yassar, A. Enzyme recognition by polypyrrole functionalized with bioactive peptides. *J. Am. Chem. Soc.* **116**, 8813–8814 (1994).
47. Kwon, O. S. *et al.* Hsp90-functionalized polypyrrole nanotube FET sensor for anti-cancer agent detection. *Biosens. Bioelectron.* **25**, 1307–1312 (2010).
48. Kwon, O. S., Park, S. J. & Jang, J. A high-performance VEGF aptamer functionalized polypyrrole nanotube biosensor. *Biomaterials* **31**, 4740–4747 (2010).
49. Kwon, O. S. *et al.* Multidimensional conductingpolymer nanotubes for ultrasensitive chemical nerve agent sensing. *Nano Lett.* **12**, 2797–2802 (2012).
50. Yoon, H. *et al.* Polypyrrole nanotubes conjugated with human olfactory receptors: high-performance transducers for FET-type bioelectronic noses. *Angew. Chem. Int. Edit.* **48**, 2755–2758 (2009).
51. Korri-Youssoufi, H., Garnier, F., Srivastava, P., Godillot, P. & Yassar, A. Toward bioelectronics: specific DNA recognition based on an oligonucleotide-functionalized polypyrrole. *J. Am. Chem. Soc.* **119**, 7388–7389 (1997).
52. Oh, W.-K., Kim, S., Yoon, H. & Jang, J. Shape-dependent cytotoxicity and proinflammatory response of poly (3, 4-ethylenedioxythiophene) nanomaterials. *Small* **6**, 872–879 (2010).
53. Chang, J. C., Brewer, G. J. & Wheeler, B. C. A modified microstamping technique enhances polylysine transfer and neuronal cell patterning. *Biomaterials* **24**, 2863–2870 (2003).
54. Justice, J. Jr. Quantitative microdialysis of neurotransmitters. *J. Neurosci. Methods* **48**, 263 (1993).
55. O'Neill, R. D. Sensor–tissue interactions in neurochemical analysis with carbon paste electrodes in vivo. *Analyst* **118**, 433–438 (1993).
56. Venton, B. J. & Wightman, R. M. Psychoanalytical electrochemistry: dopamine and behavior. *Anal. Chem.* **75**, 414 A–421 A (2003).

Acknowledgments

This research was supported by the National Research Foundation of Korea (NRF) grant (No. 2011-0017125, 2013- 003890, 2013K000368), funded by the Ministry of Education, Science and Technology (MEST). We thank Sun Young Jang (Phillips Exeter Academy) for assistance of transducer of FET sensor.

Author contributions

S.J.P. and H.S.S. contributed equally to this work; S.J.P. and H.S.S. designed and performed the experiments, and wrote the manuscript; O.S.K., J.H.C., S.H.L., J.H.A., S.R.A., J.E.L. and H.Y. contributed to data collection and theoretical analysis; T.H.P. and J.J. planned and supervised the project, and wrote the manuscript. All authors edited the manuscript.

Additional information

Supplementary information accompanies this paper at http://www.nature.com/scientificreports

Competing financial interests: The authors declare no competing financial interests.

How to cite this article: Park, S.J. *et al.* Human dopamine receptor nanovesicles for gate-potential modulators in high-performance field-effect transistor biosensors. *Sci. Rep.* **4**, 4342; DOI:10.1038/srep04342 (2014).